bioRxiv preprint doi: https://doi.org/10.1101/807701; this version posted October 17, 2019. The copyright holder for this preprint (which was not certified by peer review) is the author/funder. All rights reserved. No reuse allowed without permission.

Pegasus, a small extracellular peptide regulating the short-range diffusion of Wingless

Emile G Magny[1], Jose I Pueyo[2], Sarah A Bishop[1,2], Daniel Aguilar-Hidalgo[3] and Juan Pablo Couso[1*,2]

1. Centro Andaluz de Biologia del Desarrollo, CSIC-UPO, Sevilla, Spain

2. Brighton and Sussex Medical School, University of Sussex, Brighton, UK

3. School of Biomedical Engineering, University of British Columbia, Canada. Michael Smith Laboratories, University of British Columbia, Vancouver, British Columbia, Canada

*Current address and author for correspondence.

Abstract

Small Open Reading Frames (smORFs) coding for peptides of less than 100 amino-acids are emerging as a fundamental and pervasive gene class, found in the hundreds of thousands in metazoan genomes. Even though some of these genes are annotated, their function, if any, remains unknown. Here we characterize the function of a smORF encoding a short 80 aa peptide, *pegasus* (*peg*), which facilitates Wg diffusion during the development of the *Drosophila* wing imaginal disc. During wing development, Wg has sequential functions, and in the later stages, when *peg* is strongly expressed, it patterns the presumptive wing margin. A reduction in Wg protein secretion at this stage produces effects ranging from total abolition of the wing margin to partial loss of bristles and reduction of proneural gene expression. Here we show that the Peg peptide enhances the short-range of Wg diffusion in this context, in order to produce a proper wing margin. We show that CRISPR/Cas9-mediated mutations of *pegasus* generate wing margin phenotypes, and changes in target gene expression, consistent with a role in Wg signalling. We find that Peg is secreted, and that it co-localizes and co-immunoprecipitates with Wg, suggesting that Peg directly binds Wg in order to enhance its extracellular transport and signalling, and our data from fixed and *in-vivo* Wg gradient measurements supports a model in which this diffusion enhancement may rely on the stabilization of extracellular Wg. Our results unveil a new element in the regulation of the Wg signalling pathway, and shed light on the functional consequences of the miss-regulation of

bioRxiv preprint doi: https://doi.org/10.1101/807701; this version posted October 17, 2019. The copyright holder for this preprint (which was not certified by peer review) is the author/funder. All rights reserved. No reuse allowed without permission.

Wg diffusion in this developmental context, while also reminding us of the functional diversity, and relevance of small open reading frame genes.

Introduction

Small Open Reading Frames (smORFs) coding for peptides of less than 100 amino-acids are emerging as a fundamental and pervasive gene class, mostly uncharacterised but found in the tens of thousands in metazoan genomes (Couso and Patraquim, 2017; Ladoukakis et al., 2011) (Andrews and Rothnagel, 2014). A rich source of smORFs are the so-called long-non-coding RNAs, which several studies indicate are in fact translated in many cases (Aspden et al., 2014; Bazzini et al., 2014), and which have already been shown to produce peptides with important functions (Bhupathy et al., 2007; Galindo et al., 2007; Hanyu-Nakamura et al., 2008; Magny et al., 2013) . There is also a small number of genes annotated as coding for small peptides (short CDSs) whose function is also unknown. Their short peptides are about 80 aa long with a propensity to include both positively charged domains and hydrophobic transmembrane α-helixes (TMHS), typical of secreted and membrane-associated peptides (Aspden et al., 2014; Couso and Patraquim, 2017). Characterised shortCDS peptides localise at or near membrane organelles, and their known functions range from antimicrobial peptides (Lemaitre and Hoffmann, 2007), organelle components (Guo et al., 2003; Lee et al., 2015; Pueyo et al., 2016), and cell signals(Chng et al., 2013; Pauli et al., 2014). We identified a number of apparently translated shortCDSs in *Drosophila* for full functional characterisation, including CG17278, which we call *pegasus* (*peg*). Here, we show that *peg* encodes a secreted peptide that binds and modulates the cell signalling Wnt protein Wingless.

The development of the fly wing is a well-studied developmental system, that has lead to the characterisation of several important cell signals in animal development. Amongst these signals is the secreted *wingless/Dwnt1* protein (Wg). The Wg protein has sequential functions in fly wing development, and at the end of development it patterns the presumptive wing margin (Couso et al., 1994; Piddini and Vincent, 2009). Thus, reducing Wg protein secretion or transport with Wg mutant proteins produces effects ranging from total abolition of the wing margin to partial loss of bristles and reduction of proneural gene expression (Couso et al., 1994; Piddini and Vincent, 2009). Here, we show that the Peg peptide increases the short-range of

bioRxiv preprint doi: https://doi.org/10.1101/807701; this version posted October 17, 2019. The copyright holder for this preprint (which was not certified by peer review) is the author/funder. All rights reserved. No reuse allowed without permission.

Wg signalling by decreasing Wg degradation, and that this range enhancement is essential to establish the full extent of proneural gene activation, and hence, the full wing margin pattern.

Results

1-Identification of *peg*

peg encodes an 80 aa peptide with a signal peptide domain and a Kazal2/Follistatin-like domain (FS-like), which localised to vesicular-like cellular structures in S2 cells. FS-like domains are present in Agrin and other large heparin-sulphate proteoglycans (HSPGs). HSPGs are secreted extracellularly and bind to the extracellular matrix, facilitating the anchoring or diffusion of other proteins across it; in particular, HSPGs have been shown to promote Wnt and Hh signalling in vertebrates and flies (Hacker et al., 2005). *peg* showed good conservation in insects, and possible conservation in vertebrate genes related to the SPINK extracellular protease inhibitors (Fig. 1A). *peg* was strongly expressed in the developing fly wing but was excluded from the presumptive wing margin (Fig. 1B-C), a pattern complementary to that of the fly Wnt gene *wingless* (*wg*) (Fig. 1B-C) (Butler et al., 2003; Couso et al., 1994).

2- Characterisation of the *peg* mutant phenotype.

Available mutants for *peg* presented low viability but no overt defects. We generated null mutants by CRISPR-Cas9 producing small deletions within the coding sequence of the peptide (Fig. 1D). These mutants behave as genetic nulls and show higher pupal lethality and a significant reduction in the number of chemosensory bristles at the wing margin (Fig. 2 A,D), a characteristic phenotype of *wg* loss of function (Couso et al., 1994). The sensory organ precursors (SOPs) that give rise to chemosensory bristles are determined at the third instar larval stage of development, from cells within a proneural field induced by high levels of Wg signalling, received by a row of about 3 cells directly neighbouring the row of Wg expressing cells at the presumptive dorso-ventral boundary (Couso et al., 1994). In *peg* null mutants, the proneural marker *senseless* (*sens*) (Nolo et al., 2000) showed a significant reduction in the width of the proneural field consistent with the observed reduction of chemosensory bristles phenotype (Fig. 2B, Sup. Fig. 1 A,B). Altogether the *peg* phenotype suggests that Peg acts as a positive factor in Wg signalling.

bioRxiv preprint doi: https://doi.org/10.1101/807701; this version posted October 17, 2019. The copyright holder for this preprint (which was not certified by peer review) is the author/funder. All rights reserved. No reuse allowed without permission.

peg encodes a possible signal peptide domain, suggesting that is a secreted peptide. We looked at the expression of *sens* in *peg-/-* clones, to assess the cell autonomy of Peg, hypothesising that if Peg is indeed secreted it may act in a non-autonomous way. We also assessed the expression of Wg in order to determine if it could be a target of Peg. We observed no effect in the proneural field within small *peg* mutant clones (Fig. 2F), but in larger clones there is a loss of *sens* in cells located more than 3-4 cell diameters away from the nearest Peg-producing cells (Fig. 2E). Interestingly in these large mutant clones we also observe a reduction in extracellular Wg, while in the smaller clones with normal *sens* expression the diffusion of Wg appears normal (Fig. 2 legend: Note that intracellular Wg is always normal). These results show that Peg indeed acts in a cell non-autonomous way, consistent with its predicted secretion, with a range of some three cells. Moreover, these results show that Peg is required for proper Wg protein allocation. Due to its positive effects on Wg signalling and transport, we called this gene *pegasus* (*peg),* in analogy with the mythical winged horse that transported ancient Greek heroes.

3- Peg-GFP is functional, secreted and co-localises with Wg.

To establish the cellular localisation of Peg and its relationship with Wg *in vivo*, we generated transgenic flies expressing a *UAS-Peg-GFP* fusion (methods). Peg-GFP rescues the chemosensory phenotype of null *peg* without producing unrelated phenotypes, showing that Peg-GFP is a bona-fide replica of native Peg. We expressed Peg-GFP with *ptc-GAL4-Gal80*^{ts} in a stripe across the dorso-ventral axis and the Wg expression stripe. We observed Peg-GFP shortly after induction of its expression (5h), and by 12 hours it was detected outside this domain, showing that Peg is indeed secreted from the *ptcGal4 UAS-Peg-GFP* expressing cells (Fig. 3A, and Sup. Fig. 2). By co-expressing *UAS-Peg-GFP* and *UAS-Wg*, we found that Peg co-localises with Wg, both in expressing cells and in neighbouring ones (Fig. 3B, C). Importantly, Peg-GFP also co-localises with endogenous Wg, as corroborated when Peg-GFP is expressed throughout the wing pouch with *rn-Gal4* (Sup. Fig. 2). To test whether a direct protein-protein interaction exists between Peg and Wg we performed a co-immunoprecipitation from protein extracts of third instar larvae expressing Peg-GFP, using beads bound to anti-GFP and staining the precipitate with an anti-Wg antibody. Endogenous Wg was detected in the extract from Peg-GFP expressing larvae, but not in GFP-only expressing controls, showing that Peg can bind directly and specifically to Wg *in vivo* (Fig. 3D).

bioRxiv preprint doi: https://doi.org/10.1101/807701; this version posted October 17, 2019. The copyright holder for this preprint (which was not certified by peer review) is the author/funder. All rights reserved. No reuse allowed without permission.

4-Peg facilitates Wg transport

Having established that the Peg peptide is secreted, localizes with and binds extracellular Wg, we focused on the effect of Peg on the transport and function of extra-cellular Wg. Using *peg* mutants and the Gal4 system, we generated wings containing well-defined patterns of cells displaying presence and absence of Peg. In the absence of Peg, Wg shows a narrower range of diffusion compared to wildtype (wt) (Fig. 4 A,B F), consistent with the narrower *sens*-expressing proneural field, lack of chemosensory bristles observed in these mutants, and the lower Wg diffusion observed in large *peg-/-* clones (Fig. 2A-D). Reciprocally, when Peg-GFP was over-expressed in the posterior wing compartment by *en-GAL4*, we observed extended Wg diffusion (Fig. 4 C,F´) and Sens expression in this compartment (Fig. 4 D-E´, F´´). Peg has a similar effect on Wg-GFP diffusion and signalling, when UAS-Wg-GFP is either co- expressed with UAS-Peg, or expressed in a *peg* mutant background, using *ptc-Gal4* (see below).

If Peg has an effect on Wg transport, we reasoned that it would be possible to observe such an effect in real time *in vivo* through live imaging. We used the *ptc-GAL4-Gal80*^{ts} ; *UAS-Wg-GFP* expression system to perform Fluorescence Recovery after Photobleaching experiments *in vivo*, following a method based on the protocol of Aldaz *et al.* (Aldaz *et al*., 2010). We observe in third instar imaginal discs a recovery of 40% of the Wg fluorescence intensity by 5 minutes (Fig. 4 G,H), which suggests a very fast transport dynamics, whereas *peg* mutants show a slower rate of recovery, reaching only 14% by the same time (Fig. 4 G´,H).

5- Direct effect of Peg on Wg protein function

Our results suggest that Peg acts extracellularly and directly on Wg by enhancing its transport dynamics as required for proper wing margin patterning, including proneural gene activation. Importantly, the positive effect of Peg on Wg transport and signalling are linked and map to the Wg protein. Firstly, we carried out *in-situ* hybridisations to detect *wg* mRNA, and we did not observe an expansion of the *wg* transcription domain upon over-expression of Peg, in the posterior compartment using our *en-Gal4, UAS-peg-GFP* line (Fig. 5 F). Secondly, the correlated expansion of both Wg spatial range, and expression of the *wg*-signalling target gene *sens* is linked by a similar expansion of Armadillo (Arm) nuclear localisation, a known marker of Wg signalling activity (Fig. 5A-E). Thirdly, abolition of Wg transport is epistatic over Peg function: it has been shown that a substitution of endogenous Wg protein with a membrane-tethered version (Wg^{NRT}) gives rise to apparently morphologically normal flies (Piddini and

bioRxiv preprint doi: https://doi.org/10.1101/807701; this version posted October 17, 2019. The copyright holder for this preprint (which was not certified by peer review) is the author/funder. All rights reserved. No reuse allowed without permission.

Vincent, 2009). We looked in detail at the Wg margin patterning and *sens* expression in these Wg^{NRT} flies and found similar phenotypes as those of *peg* mutants (Fig. 5G-H´), which over-expression of Peg was not able to rescue, and which loss of function of *peg* did not enhance.

Overall our results show that Peg promotes Wg transport on the one hand, while on the other hand Peg promotes Wg signalling acting upstream or on the Wg protein itself. The simplest hypothesis is that both effects are causally linked, such that the Peg peptide facilitates Wg protein transport, which in turn results in expanded Wg signalling and expression of target genes. Thus, our results corroborate that a local spatial range of Wg of 3-4 cells is required for proper establishment of the wing margin and its associated proneural field (Couso et al. 1994), and that reducing Wg transport by either Peg loss or Wg tethering results in a reduction of these developing structures.

6-Effect of Peg on Wg stability

Since Peg has a predicted domain which has been associated with both protease inhibition activity (Guy et al., 1971; Rimphanitchayakit and Tassanakajon, 2010), and HSPGs, we asked whether Peg may have an effect in Wg stability / degradation (working as a protease inhibitor), or in its extracellular movement (working as an HSPG). Using the data from our Wg-GFP gradients in wt and $peg^{-/-}$ mutant conditions, and from our *in vivo* Wg diffusion experiments, we formalize the effective transport dynamics of Wg with a simple reaction diffusion model (see methods), $\partial C/\partial t = D\partial^2 C/\partial x^2 - KC + \upsilon$, where C is the Wg ligand concentration, which is a function of time and space, D is the effective diffusion coefficient, K is the effective degradation rate and ν is the ligand source rate, which is spatial dependent. Within this model, we can define a length scale that indicates the decay in concentration for a constant source width, and the length of the tissue in the direction perpendicular to the source being much longer than the decay-length of the gradient, the solution of this equation in steady state is an exponential form $C(x) = C_0 e^{-x/\lambda}$ where C_0 is the amplitude (intensity) of the gradient at the target tissue right next to the source, and λ is the decay length of the gradient, which is a function of D and K. With this method and our imaging data, we obtained similar diffusion coefficients between peg-/- and wt ; $D_{wt} = 0.38 \pm 0.30$ µm^2/s and $D_{peg-/-} = 0.46 \pm 0.16$ µm^2/s, but we found a significant change in the decay length between these conditions; $\lambda_{wt} = 5.90 \pm 0.20$ µm, $\lambda_{peg-/-} = 3.16 \pm 0.34$ µm, which can be explained by a difference in the effective degradation rate of the ligand: $K_{wt} = 0.011 \pm 0.008$ /s, $K_{peg-/-} = 0.051 \pm 0.006$ /s. These results

bioRxiv preprint doi: https://doi.org/10.1101/807701; this version posted October 17, 2019. The copyright holder for this preprint (which was not certified by peer review) is the author/funder. All rights reserved. No reuse allowed without permission.

imply that in *peg*$^{-/-}$ Wg is degraded faster, leading to the observed shortening in the decay-length of the mutant gradient. In wt conditions Wg appears to be more stable, and with a smaller effective degradation rate. To corroborate this solution, we measured directly the levels of mRNA and protein using qRT-PCR and quantitative Western blots, respectively. Consistent with the *in-situ* hybridisation data, we observed no significant changes in mRNA transcript levels when *peg* was over-expressed. However, Peg over-expression in the wing imaginal disc pouch led to significantly higher levels of Wg protein compared to controls expressing GFP-only, and to wt discs.

Altogether our cellular, biochemical and mathematical data support a role for Peg as a facilitator of Wg transport by stabilizing extracellular Wg, possibly, given its close evolutionary relationship to the family of serine protease inhibitors of the Kazal-type, by limiting its degradation through the inhibition of (a) yet unidentified protease(s). To our knowledge, this is the first data on Wg extracellular degradation, a crucial component of any gradient dynamics (Aguilar-Hidalgo et al., 2019; Kicheva et al., 2007).

Discussion:

Although Wg has been characterised as a diffusible ligand, acting on a range of several cells, it was reported that the substitution of the *wg* locus by a membrane tethered version of Wg (NRT-Wg) gives rise to flies that develop apparently normally (although poorly viable), with no overt morphological phenotypes, suggesting that a long range action by diffusion of Wg may not be required during development (Piddini and Vincent, 2009). However, some studies using the NRT-Wg *Drosophila* line have shown that Wg signalling at a distance is required in specific contexts (Beaven and Denholm, 2018). Here we show that short-range diffusion of Wg is indeed required for the appropriate patterning of the wing margin, as initially reported. We showed how the Wg/Wnt1 protein has sequential short range signalling functions in Drosophila wing development, instead of a single, long range morphogenetic function, a crucial fact that reconciles results from several groups (Couso et al., 1993a; Couso et al., 1994; Couso et al., 1995; Klein and Martinez Arias, 1999) (Sup. Fig 3). Thus, early in wing development Wg establishes a 10-cell wide wing field from the ventral compartment; Wg perturbations at this stage result in either loss of the entire wing, or its duplication (Couso et al., 1993a; Couso et al., 1995; Klein, 2001; Neumann and Cohen, 1997). Shortly afterwards, transitory expression of Wg across the entire developing wing is required for wing growth (Couso et al.,1993;

bioRxiv preprint doi: https://doi.org/10.1101/807701; this version posted October 17, 2019. The copyright holder for this preprint (which was not certified by peer review) is the author/funder. All rights reserved. No reuse allowed without permission.

Neumann and Cohen, 1996; Piddini and Vincent,2009; Couso and Martinez Arias1994), and finally, Wg is expressed in a stripe along the dorsal-ventral boundary of the wing from where it patterns the wing margin (Couso et al. 1994). The widespread growth function does not strictly require Wg diffusion (since Wg is then transcribed in nearly all cells of the developing wing) but the other two functions rely on effective short-range Wg signalling. The early establishment of the wing field occurs in a primordia 10 cells across, yet its effects are eventually and indirectly felt across hundreds of cells by the end of development; whereas the late patterning of the wing margin offers a direct read-out of the functional range of Wg signalling. In this late context involving a short-range Wg signal, the Peg peptide is an essential part of Wg transport. Peg enhances Wg transport to reach cells located 3-4 cell diameters from the Wg source, which otherwise would be deprived of the Wg signal. The signalling to the entire proneural field is essential to ensure the development of all the neural precursors and bristles that the wing margin displays, in particular the number of chemoreceptors that inform the fly of its surroundings, and the subsequent positioning of the mechanoreceptors that allow the fly to keep steady constant flight. Our results show that Peg enhances Wg transport by increasing its stability, possibly by inhibiting its degradation, highlighting control of degradation as an essential component of signalling gradients: extreme degradation would preclude signalling to cells not in direct contact, and no degradation would lead to the ligand ‘filling up’ the receiving tissue.

Our results also corroborate the growing importance of smORFs. Given their numbers and molecular characteristics, it is likely that more smORFs of importance in development and inter-cellular communication await characterisation across metazoans. Further, at the genomic level, smORFs could well represent emerging new genes in our genomes (Couso and Patraquim, 2017). Only continued smORF studies will uncover the true answers to their potential.

bioRxiv preprint doi: https://doi.org/10.1101/807701; this version posted October 17, 2019. The copyright holder for this preprint (which was not certified by peer review) is the author/funder. All rights reserved. No reuse allowed without permission.

References:

Aguilar-Hidalgo, D., Hadjivasilou, Z., Romanova-Michaelides, M., González-Gaitán, M., Jülicher, F., 2019. Dynamic modes of morphogen transport. arXiv arXiv:1909.13280.

Aldaz, S., Escudero, L.M., Freeman, M., 2010. Live imaging of Drosophila imaginal disc development. Proc Natl Acad Sci U S A 107, 14217-14222.

Andrews, S.J., Rothnagel, J.A., 2014. Emerging evidence for functional peptides encoded by short open reading frames. Nat Rev Genet 15, 193–204.

Aspden, J.L., Eyre-Walker, Y.C., Philips, R.J., Brocard, M., Amin, U., Couso, J.P., 2014. Extensive translation of small Open Reading Frames revealed by Poly-Ribo-Seq eLife 3, e03528.

Bazzini, A.A., Johnstone, T.G., Christiano, R., Mackowiak, S.D., Obermayer, B., Fleming, E.S., Vejnar, C.E., Lee, M.T., Rajewsky, N., Walther, T.C., Giraldez, A.J., 2014. Identification of small ORFs in vertebrates using ribosome footprinting and evolutionary conservation, EMBO J, 2014/04/08 ed, pp. 981-993.

Beaven, R., Denholm, B., 2018. Release and spread of Wingless is required to pattern the proximo-distal axis of Drosophila renal tubules. Elife 7.

Bhupathy, P., Babu, G.J., Periasamy, M., 2007. Sarcolipin and phospholamban as regulators of cardiac sarcoplasmic reticulum Ca2+ ATPase. J Mol Cell Cardiol 42, 903-911.

Butler, M.J., Jacobsen, T.L., Cain, D.M., Jarman, M.G., Hubank, M., Whittle, J.R., Phillips, R.G., Simcox, A.A., 2003. Discovery of genes with highly restricted expression patterns in the Drosophila wing disc using DNA oligonucleotide microarrays. Development 130, 659-670.

Chng, S.C., Ho, L., Tian, J., Reversade, B., 2013. ELABELA: a hormone essential for heart development signals via the apelin receptor. Dev Cell 27, 672-680.

Couso, J.P., Bate, M., Martinez-Arias, A., 1993a. A wingless-dependent polar coordinate system in Drosophila imaginal discs. Science 259, 484-489.

Couso, J.P., Bate, M., Martinez Arias, A., 1993b. A wingless-dependent polar coordinate system in Drosophila imaginal discs. Science 259, 484-489.

Couso, J.P., Bishop, S.A., Martinez Arias, A., 1994. The wingless signalling pathway and the patterning of the wing margin in Drosophila. Development 120, 621-636.

Couso, J.P., Knust, E., Martinez Arias, A., 1995. Serrate and wingless cooperate to induce vestigial gene expression and wing formation in Drosophila. Curr Biol 5, 1437-1448.

Couso, J.P., Patraquim, P., 2017. Classification and function of small open reading frames. Nat Rev Mol Cell Biol 18, 575-589.

Diaz-Benjumea, F.J., Cohen, S.M., 1993. Interaction between dorsal and ventral cells in the imaginal disc directs wing development in Drosophila. Cell 75, 741-752.

Galindo, M.I., Pueyo, J.I., Fouix, S., Bishop, S.A., Couso, J.P., 2007. Peptides encoded by short ORFs control development and define a new eukaryotic gene family. PLoS Biology 5, 1052-1062.

Gonzalez, F., Swales, L., Bejsovec, A., Skaer, H., Martinez Arias, A., 1991. Secretion and movement of wingless protein in the epidermis of the Drosophila embryo. Mech Dev 35, 43-54.

Guo, B., Zhai, D., Cabezas, E., Welsh, K., Nouraini, S., Satterthwait, A.C., Reed, J.C., 2003. Humanin peptide suppresses apoptosis by interfering with Bax activation. Nature 423, 456-461.

Guy, O., Shapanka, R., Greene, L.J., 1971. The structure of the bovine pancreatic secretory trypsin inhibitor--Kazal's inhibitor. 3. Determination of the disulfide bonds and proteolysis by thermolysin. J Biol Chem 246, 7740-7747.

Hacker, U., Nybakken, K., Perrimon, N., 2005. Heparan sulphate proteoglycans: the sweet side of development. Nat Rev Mol Cell Biol 6, 530-541.

bioRxiv preprint doi: https://doi.org/10.1101/807701; this version posted October 17, 2019. The copyright holder for this preprint (which was not certified by peer review) is the author/funder. All rights reserved. No reuse allowed without permission.

Hanyu-Nakamura, K., Sonobe-Nojima, H., Tanigawa, A., Lasko, P., Nakamura, A., 2008. Drosophila Pgc protein inhibits P-TEFb recruitment to chromatin in primordial germ cells. Nature 451, 730-733.

Kicheva, A., Pantazis, P., Bollenbach, T., Kalaidzidis, Y., Bittig, T., Julicher, F., Gonzalez-Gaitan, M., 2007. Kinetics of morphogen gradient formation. Science 315, 521-525.

Klein, T., 2001. Wing disc development in the fly: the early stages. Curr Opin Genet Dev 11, 470-475.

Klein, T., Arias, A.M., 1998. Different spatial and temporal interactions between Notch, wingless, and vestigial specify proximal and distal pattern elements of the wing in Drosophila. Dev Biol 194, 196-212.

Klein, T., Martinez Arias, A., 1999. The vestigial gene product provides a molecular context for the interpretation of signals during the development of the wing in Drosophila. Development 126, 913-925.

Ladoukakis, E., Pereira, V., Magny, E.G., Eyre-Walker, A., Couso, J.P., 2011. Hundreds of putatively functional small open reading frames in Drosophila. Genome Biol 12, R118.

Lee, C., Zeng, J., Drew, B.G., Sallam, T., Martin-Montalvo, A., Wan, J., Kim, S.J., Mehta, H., Hevener, A.L., de Cabo, R., Cohen, P., 2015. The mitochondrial-derived peptide MOTS-c promotes metabolic homeostasis and reduces obesity and insulin resistance. Cell metabolism 21, 443-454.

Lemaitre, B., Hoffmann, J., 2007. The host defense of Drosophila melanogaster. Annu Rev Immunol 25, 697-743.

Magny, E.G., Pueyo, J.I., Pearl, F.M., Cespedes, M.A., Niven, J.E., Bishop, S.A., Couso, J.P., 2013. Conserved regulation of cardiac calcium uptake by peptides encoded in small open reading frames. Science 341, 1116-1120.

Neumann, C.J., Cohen, S.M., 1997. Long-range action of Wingless organizes the dorsal-ventral axis of the Drosophila wing. Development 124, 871-880.

Nolo, R., Abbott, L.A., Bellen, H.J., 2000. Senseless, a Zn finger transcription factor, is necessary and sufficient for sensory organ development in Drosophila. Cell 102, 349-362.

Pauli, A., Norris, M.L., Valen, E., Chew, G.L., Gagnon, J.A., Zimmerman, S., Mitchell, A., Ma, J., Dubrulle, J., Reyon, D., Tsai, S.Q., Joung, J.K., Saghatelian, A., Schier, A.F., 2014. Toddler: an embryonic signal that promotes cell movement via Apelin receptors. Science 343, 1248636.

Phillips, R.G., Whittle, J.R., 1993. wingless expression mediates determination of peripheral nervous system elements in late stages of Drosophila wing disc development. Development 118, 427-438.

Piddini, E., Vincent, J.P., 2009. Interpretation of the wingless gradient requires signaling-induced self-inhibition. Cell 136, 296-307.

Pueyo, J.I., Magny, E.G., Sampson, C.J., Amin, U., Evans, I.R., Bishop, S.A., Couso, J.P., 2016. Hemotin, a regulator of phagocytosis encoded by a small ORF and conserved across metazoans. PloS Biology 14, e1002395.

Rimphanitchayakit, V., Tassanakajon, A., 2010. Structure and function of invertebrate Kazal-type serine proteinase inhibitors. Dev Comp Immunol 34, 377-386.

St Pierre, S.E., Galindo, M.I., Couso, J.P., Thor, S., 2002. Control of Drosophila imaginal disc development by rotund and roughened eye: differentialy expressed transcripts of the same gene encoding functionally distinct zinc finger proteins. Development 129, 1273-1281.

bioRxiv preprint doi: https://doi.org/10.1101/807701; this version posted October 17, 2019. The copyright holder for this preprint (which was not certified by peer review) is the author/funder. All rights reserved. No reuse allowed without permission.

Materials and methods:

Drosophila lines:

Fly stocks and crosses were cultured at 25 ^{0}C, unless otherwise stated. For induction of gene expression with the Gal4, Gal80^{ts} system, the cultures were carried out at 18°C and then shifted to 29°C prior to dissection. The following lines were obtained from the *Drosophila* Bloomington stock centre at Indiana University: *Or-R (used as wt)***,** *w;; Mi(MIC)02608, w;;Df(3R)BSC680, w;;69B-Gal4, w;;UAS-dsRed, w;en-Gal4,UAS-dsRed /CyO, w hsFlp;; FRT 82B tub-GFP*. *The w;ptc-Gal4-UAS-Gal80^{ts} ;MKRS/TM6b* was a gift from James Castelli Gair-Hombria, the *w; UAS-wg-GFP* and *w; wg-NRT stocks* were gifts from Jean Paul Vincent. *rn-Gal4^{13}* was previously published in St Pierre *et al. 2002.*

Transgenic constructs:

To generate the *peg-GFP* construct, a fragment containing the *CG17278* 5' UTR and CDS sequences (devoid of stop codon) was amplified from a whole *Drosophila* embryo cDNA library and cloned into a TOPO-TA gateway pEntry vector, this vector was then recombined with the pPWG vector (UAS-insert-C terminal GFP), obtained from the *Drosophila Genomics Resource Centre at Indiana University*, to obtain *UAS-peg-GFP*. The *UAS-peg-GFP* plasmid was then sent to BESTgene for injection into embryos and generation of transgenic flies.

Generation of CRISPR mutants:

To generate the *peg $^{-/-}$* null mutants we cloned the following guide sequence targeting the CDS of CG17278: GTACCGATCCATTTGCGCTGCGG into the *pU6-BbsI-chiRNA* plasmid, obtained from *addgene*, and following the available protocol (http://FlyCRISPR.molbio.wisc.edu). The following primers were used: *chi-CG17278 ORF guide 1 Fw* CTTCGTACCGATCCATTTGCGCTG and *chi-CG17278 ORF guide 1* Rv AAACCAGCGCAAATGGATCGGTAC. The *pU6-CG17278-chiRNA* plasmid was then sent for injection to BESTgene into the y[1] M{vas-Cas9}ZH2A w[1118] line. Surviving adults were crossed to *w;;Df(3R)BSC680*, the progeny was scored for *peg-/-* like phenotypes, stocks were established from putative *peg* mutants, and *peg* alleles were confirmed by PCR of the locus followed by sequencing.

Wing preparations:

For Drosophila adult wing preparations, the flies were collected in SH media (50% glycerol, 50% ethanol), washed in ethanol and then in dH2O, then wings were then clipped and mounted on a slide with Hoyer´s. The slides were then placed in a hot plate at 65°C for 3-5 hours, with a weight on top of the coverslip to ensure a good flattening of the wings.

In situ hybridization:

CG17278 ribo-probe was obtained using the *CG1728 in pEntry* plasmid and its T3 promoter, and the *wg* ribo-probe was obtained from a whole wg cDNA fragment in pBluescript, which

bioRxiv preprint doi: https://doi.org/10.1101/807701; this version posted October 17, 2019. The copyright holder for this preprint (which was not certified by peer review) is the author/funder. All rights reserved. No reuse allowed without permission.

was a gift from Joaquin Culi Espigul and Sol Sotillos, it was transcribed using its T3 promoter. Digoxigenin labelling of the ribo-probes was performed with the *Roche DIG RNA labelling mix, Sigma Aldrich*, and the *Promega* T3 RNA polymerase. Wing imaginal discs were dissected in ice-cold PBS and fixed for 20 minutes in 4% paraformaldehyde, and a standard DIG-RNA *in situ* hybridization protocol, as described in Galindo e*t al.* 2007, was followed.

Antibody stainings:

For wing imaginal disc immuno-stainings, wandering third instar L3 larvae were dissected by evertion in ice-cold PBS, cleared of digestive system and fat body, fixed for 15 minutes in 4% pfa, and left overnight in methanol at -20ºC. The tissues were then washed 3 times with PBS. For wingless stainings, a single wash of 20 minutes with PBS, Tween (0.1%) was performed and the rest of the incubations and washes were carried out with ice cold PBS, BSA (0.2%), and ice cold PBS, respectively, maintianing detergent-free conditions in order to preserve the extracellular signal. Anti-Wg 4D4 (mouse, used at 1:50) and anti-Arm 7A1 (mouse, used 1:50) were obtained from *The Developmental Studies Hybridoma Bank*, at the *University of Iowa.* Anti-Sens (Guinea-Pig, used 1:3000) was a gift from Takashi Koyama. We used the following secondary antibodies: to detect Wg we used anti-mouse biotin, Jackson (1:200), and avidin-Cy5 or avidin-FITC, Jackson, (1:1000) or (1:500) respectively, for other antigens we used anti mouse-Rhodamine, jackson (1:250), and anti guinea-pig-rhodamine, Jackson, (1:250). For nuclear labelling we used DAPI at a final concentration of 300 nM.

Confocal images were acquired on a Zeiss Axio Observer microscope, with an LSM 880 Airyscan module, using a 63x/1.46 oil objective. The signal from Wg, Wg-GFP, Peg-GFP, Arm, and Sens, were always detected using the Airyscan detector. The signal from DAPI and UAS-GFP, or dsRED was detected using the GAasp detectors.

-Induction of peg and wg-GFP

In order to induce the expression of Wg-GFP and Peg-GFP, *Drosophila* lines of the appropriate genetic backgrounds were crossed to lines carrying *ptc-Gal4-UAS-Gal80*^{ts} , the progeny was reared at 18ºC for aproximately 168h and then shifted to 30ºC for 24h. After the shift wandering L3 larvae were collected, dissected in ice cold PBS and fixed in 4% pfa. The rearing and shift times were modified as necessary for the 5h, 8h, 12h, and 48h shifts.

-Fluorescence Signal intensity measurements

For endogenous Wg, the signal was quanitified by counting the total number of Wg particles on 15 successive 2.5 micron ROIs, centred on the D/V boundary. Raw images were thresholded and the particle analyser plugin of image J used to obtain the number of particles/ROI. For Induced Wg expression in the *ptc*-expression domain, the fluorescence signal profile was measured within a 20 µm^2 ROI on the posterior domain, placed directly adjacent to the *ptc* domain. The Sens fluorescence signal profiles were measured within a region of interest (ROI) of 20 X 60 µm, from the centre of the d/v boundary outwards, on either side of the d/v boundary.

bioRxiv preprint doi: https://doi.org/10.1101/807701; this version posted October 17, 2019. The copyright holder for this preprint (which was not certified by peer review) is the author/funder. All rights reserved. No reuse allowed without permission.

For Arm nuclear signal quantification, we calculated the ratio of total Arm signal overlapping with DAPI, with that of membrane Arm (not overlapping with DAPI).

-*in vivo* time lapse imaging

For *in-vivo* time lapse imaging of Wg-GFP diffusion, after induction of expression, we dissected the imaginal discs from wandering L3 larvae of the appropriate genotypes, in ice cold Schneider's culture medium. The imaginal discs were then transferred to an imaging chamber similar to that used in *Aldaz et al. 2010;* the chamber was constructed by sticking a perforated square of double sided tape on the cover-slip of a cover-slip bottomed culture well (*MatTek Corp*), the orifice of the perforated tape was filled with culture media (Schneider's media, 2% FBS, 0.2% Penicillin-Streptomycin, 1.25 mg/mL insulin, and 2.5% methyl-cellulose as thickener to reduce drifting of the tissues during imaging). For confocal imaging, 7 section z-stacks were acquired at a rate of a whole stack every 30 seconds, using the LSM 880 Airyscan module of the Zeiss Axio Observer microscope, with a 63x/1.46 oil objective, bleaching was performed after the first stack, by 25 iterations with the 405nm Laser line, at 80% power, in a ROI of 15 X 45nm, placed at an average of 0.5nm from the wg-GFP source. Fluorescence intensity measurements were performed on raw image files, using image J. In order to quantify the fluorescence recovery, we calculated the percentage of the original intensity (pre-bleach) recovered, after bleaching, for each time point, hence the following normalization for each data point: Intensity(t_X)=(Intensity(t_x)- Intensity (t_{bleach}))*100/ intensity ($t_{pre\text{-}bleach}$).

FRT-mediated clone generation:

In order to obtain *peg*$^{-/-}$ mitotic clones, we generated a *w; ; peg* $^{Del\ 1}$ *FRT82B* recombinant line using the *w hsFlp;; FRT 82B tub-GFP* line as the source of FRT82B. These two lines were crossed, and a 1h 37ºC heat shock was induced in the progeny 24h after egg laying.

Co-immuno precipitation:

60 late third instar larvae per genotype (*da-Gal4*, *UAS-Peg-GFP* or *UAS-GFP*) were homogenized in 400 µl of lysis buffer (20mM Tris-HCl pH 7.4/150mM NaCl/1mM EDTA/ 0.5% NP-40) for 30 min (4ºC). Cellular debris was spun at 13 000 rpm for 10 min at 4ºC. Supernatant was added to equilibrated GFP-beads (Chromo Tek, NY, USA) and left rotating overnight at 4ºC. Beads were washed three times with washing buffer (20mM Tris-HCl pH 7.4/150 mM NaCl/1mM EDTA), and then boiled in Laemmi Loading Buffer (Biorad, CA, USA). Beads were loaded onto 8 or 12% polyacrylamide gel and proteins were separated by SDS-PAGE (Biorad). Detection of specific proteins by Western Blot using a semidry blotting or tetra cell (Biorad). Antibodies used were: mouse anti-GFP 1:2500 (Roche); anti-wg 1:000 (DSHB).

Quantitative Western blot:

For each WB lane, 10 wing imaginal discs were homogenised in 20µL of LB2x Buffer (100 mM Tris-HCl pH 6.8, 4% SDS, 0.005% Bromophenol Blue, 20% Glycerol), incubated 5 minutes at 90ºC, and centrifuged at 13000 rpm for 5 minutes. The whole lysates were loaded on a Stain Free tgx acrylamide gel (*BioRad*). The proteins were transferred onto a nitrocellulose membrane, with a Trans Blot Turbo Transfer System (*BioRad*) (7 minutes, 1.3A, limited to 25V). Total protein loads were quantified before and after transference, using the

bioRxiv preprint doi: https://doi.org/10.1101/807701; this version posted October 17, 2019. The copyright holder for this preprint (which was not certified by peer review) is the author/funder. All rights reserved. No reuse allowed without permission.

Image Lab suite (BioRAD). Wg was detected with anti Wg 4d4 (mouse, DSHB, 1:3000) and anti-mouse-HRP (Jackson, 1:10000), using the ECL select reagent (GE Healthcare) and the Chemidoc MP imager (*BioRad*). Quantification of protein levels were performed against total protein loads for each lane.

Quantitative real time reverse transcriptase PCR:

Total mRNA was extracted from 30 imaginal discs per genotype, using the RNeasy mini kit (*Quigen*). For each sample, 500ng of mRNA was used for the reverse-transcriptase reaction, using the Quantitect reverse transcriptase kit (*Quigen*). The qPCRs were performed on a CFX connect thermocycler (*Biorad*) using the Vazyme AceQ SYBR qPCR Master Mix in 20 uL reactions, and using the following primers: Wg fw CCAAGTCGAGGGCAAACAGAA ; Wg rv TGGATCGCTGGGTCCATGTA; rp49 fw AGCATACAGGCCCAAGATCG; rp49 rv TGTTGTCGATACCCTTGGGC.

Homology searches:

For homology searches and phylogenetic analyses we used the same methods as described in (Magny et al., 2013).

bioRxiv preprint doi: https://doi.org/10.1101/807701; this version posted October 17, 2019. The copyright holder for this preprint (which was not certified by peer review) is the author/funder. All rights reserved. No reuse allowed without permission.

Figures and Figure legends;

Figure 1

A. Phylogenetic tree and alignments of different proteins with FS-like domains (including Peg, the large secreted proteoglycans Agrin and Testican, and the family of small secreted Serine Protease Inhibitors of the Kazal type (Spinks)). Note the closer relationship between Peg and zPeg, a putative Peg homologue in zebrafish. Note also that the Fs-like domain of the protease-inhibitory Spink family shows a highly conserved pattern of cysteines (highlighted in red), whereas the pattern in Peg resembles more that of the non-inhibitory proteoglycans. The signal peptide and FS-like domains are indicated in blue and pink, respectively.

B-C. *In-situ* hybridization showing the patterns of expression of *wg* and *peg* in mid (B, B´) and late (C, C´) third instar wing imaginal discs. *peg* is strongly expressed in the wing pouch, but not in the cells of the presumptive wing margin (arrows), where Wg is expressed at these stages.

D. Diagram showing the genomic site targeted for CRISPR/Cas9 mutagenesis, the DNA and protein sequence of the generated null alleles Del1 and 2, and the Kazal domain.

Figure 2

A. *peg* mutants (A´) present a reduction in wing margin sensory organs (dorsal chemo-sensory bristles (*)) compared to wild type (A).

B. The expression of *sens* in late third instar wing imaginal discs shows a reduction in *peg* mutant flies (B´) compared to wt (B). Note the the unaffected twin campaniform sensila (tsm) precursor in both images.

C. *In-situ* hybridization showing that *peg* null mutants (C´) present no changes in Wg mRNA expression compared to wt (C).

D. Quantification of chemosensory bristles in different genetic backgrounds. *peg* mutants show a significant reduction compared to wild-type. This phenotype is rescued by expression of Peg-GFP. Flies homozygous for a membrane bound version of Wg (Nrt-Wg) show a similar, albeit stronger, phenotype, which is not rescued by over-expression of Peg-GFP.

E-E´´. Large *peg* mutant clones (labelled by absence of GFP, green) show a reduction in *sens* expression (red) and in extracellular Wg (blue dots) present outside the wg-expressing cells ((blue intracellular staining, which remains normal in the clone). Within these large clones, mutant cells neighbouring wild-type cells have a near-normal expression of *sens* and extracellular Wg (Arrowheads).

F-F´´Small clones (up to 6 cell diameters wide) show no reduction in either *sens* expression (F,F´) or Wg diffusion (F,F´´) (arrows). Note that intracellular Wg is always normal.

bioRxiv preprint doi: https://doi.org/10.1101/807701; this version posted October 17, 2019. The copyright holder for this preprint (which was not certified by peer review) is the author/funder. All rights reserved. No reuse allowed without permission.

Figure 3

A. Induction of Peg-GFP expression with *ptc-Gal4-UAS-Gal80^{ts}* by temperature shift (18°C to 29°C) prior to dissection shows that Peg-GFP (green) is secreted. (A) Without temperature shift no GFP expression is detectable; (A´) after a brief 5h shift, GFP signal becomes detectable in the *ptc* expression domain; (A´´) 12 hours after temperature shift, secreted Peg-GFP can be detected outside of the *ptc* expression domain (labelled with Ds-red).

B. When co-induced, Peg-GFP and Wg, are similarly secreted from the *ptc* expression domain, and show extensive co-localisation (arrowheads). Temperature shift 12h prior to dissection.

C. Orthogonal view of (B), highlighting the co-localisation between Peg-GFP and Wg (arrowheads).

D. Endogenous Wg co-immunoprecipitates with Peg-GFP, but not with GFP-only controls, showing that a specific direct protein-protein interaction exists between Peg and Wg.

Figure 4

A-C. Wg diffusion is reduced in *peg* mutant wing imaginal discs (B) compared to *wt* (A), and it is enhanced in the posterior compartment when *peg-GFP* expression is driven by posterior-specific driver *en-Gal* (C).
D-E´. Over-expression of Peg-GFP in the posterior compartment (D-D´) leads to a compartment-specific increase in *sens* expression, compared to control imaginal discs over-expressing GFP-only with the same driver (E-E´). tsm, twin campaniform sensila.
F. Quantification of Wg (F,F´) and Sens (F´´) signal intensity from panels A-E´´. (F, F´) quantification of the average number of fluorescent Wg particles per µm^2 on either side of the presumptive wing margin center (line at 0 µm). (F) wing discs of wt flies show significantly higher number of fluorescent particles, further away from the center than those of *peg-/-* mutants. (F´) The posterior compartment of *en-Gal4, UAS-peg-GFP* wing discs show a significantly higher number of fluorescent particles further away from the center than the anterior compartment in the same wing discs. (F´´) The posterior compartment of *en-Gal4, UAS-peg-GFP* wing discs show significantly higher levels of Sens signal than the posterior compartment of *en-Gal4, UAS-GFP* controls.
G-G´. *In-vivo* imaging showing Wg-GFP before (pre), immediately after (t0, bleach), 30s, and 5 min after photo-bleaching (performed on indicated region within white squares), in a wild-type (G) or a *peg* mutant (G´) background. Note the much slower recovery of GFP signal in the *peg* mutant background. Expression was induced 24h prior to dissection.
H. Quantification of the fluorescence recovery from the experiments shown in panels G-G´, showing the average fluorescence intensity within the bleached region, over time, and relative to the fluorescent intensity before bleaching (pre). Acquisition was made every 30s. t0 indicates the time immediately after bleaching.

bioRxiv preprint doi: https://doi.org/10.1101/807701; this version posted October 17, 2019. The copyright holder for this preprint (which was not certified by peer review) is the author/funder. All rights reserved. No reuse allowed without permission.

Figure 5

A-A´´. Induction of Wg-GFP expression with *ptc-Gal4-UAS-Gal80^{ts}* by temperature shift 12 h before dissection in a *peg* mutant background (A), a wt background (A´), or in co-induction with Peg *(A´´).* Diffusion is reduced in a *peg* mutant background, and enhanced when Wg is co-expressed with Peg.

B-B´´. High magnification of the cells neighbouring Wg expressing cells (yellow rectangles in (A-A´´)), stained with anti-Armadillo (red) and DAPI (blue). Nuclear Armadillo levels are reduced in *peg* mutants (B), and enhanced in wing discs co-expressing Peg *(B´´)* compared *to wt (B´).*

C-D´´. Lower magnification images showing non-membrane accumulation of Armadillo (red) in the cells near Wg-GFP (green) expression in *peg* mutant (C, D), wild-type (C´,D´), and Peg over-expression backgrounds. Accumulation of Arm is lowest in the absence of Peg, and highest when it is overexpressed.

E. Quantification of the ratio of signal from nuclear/membrane Armadillo from panels B-B´´.

F-F´. *In-situ* hybridization showing *wg (*F*)* or *peg* (F´) mRNA expression when *peg-GFP* is over-expressed in the posterior compartment. *peg* over-expression is noticeable as the probe hybridizes both endogenous *peg* and induced *peg-GFP* mRNAs, yet it has no effect in Wg mRNA expression. *a* and *p* indicate anterior and posterior compartments.

G-G´. In *wg-NRT* homozygous discs (G) Wg (green) localises to the cell-membrane, and fails to diffuse away from the expressing cells. In these discs there is a strong reduction in *sens* expression (red) compared to wild type (G´). tsm, twin campaniform sensila precursor.

H-H´. *wg-NRT* homozygous flies (H) have a "narrow double row" phenotype (Couso et al. 1994) presenting a reduction in slender chemosensory bristles (*) and stout mechanosensory receptors (sometimes replaced by remaining chemosensory bristles, arrowhead). Over expression of *peg-GFP* in the wing imaginal disc using the *69B-Gal4* driver (H´), or using a *peg* -/- background (H´´) does not affect the *wg-NRT* wing margin phenotype, (See Fig. 2D for quantification). Flies homozygous for the *wg^{IL}* temperature sensitive allele, grown at the permissive 17°C temperature, show a similar lack of bristles phenotype (I), interestingly this allele has been shown to affect Wg secretion(Couso et al., 1994; Gonzalez et al., 1991).

bioRxiv preprint doi: https://doi.org/10.1101/807701; this version posted October 17, 2019. The copyright holder for this preprint (which was not certified by peer review) is the author/funder. All rights reserved. No reuse allowed without permission.

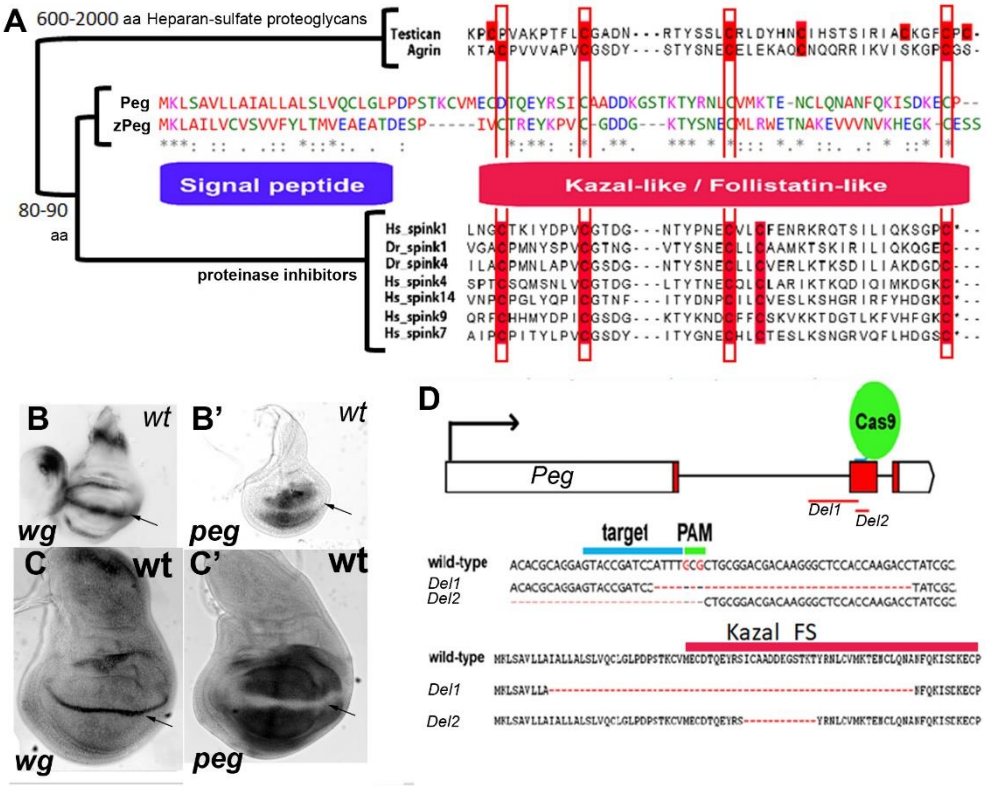

Figure 1

bioRxiv preprint doi: https://doi.org/10.1101/807701; this version posted October 17, 2019. The copyright holder for this preprint (which was not certified by peer review) is the author/funder. All rights reserved. No reuse allowed without permission.

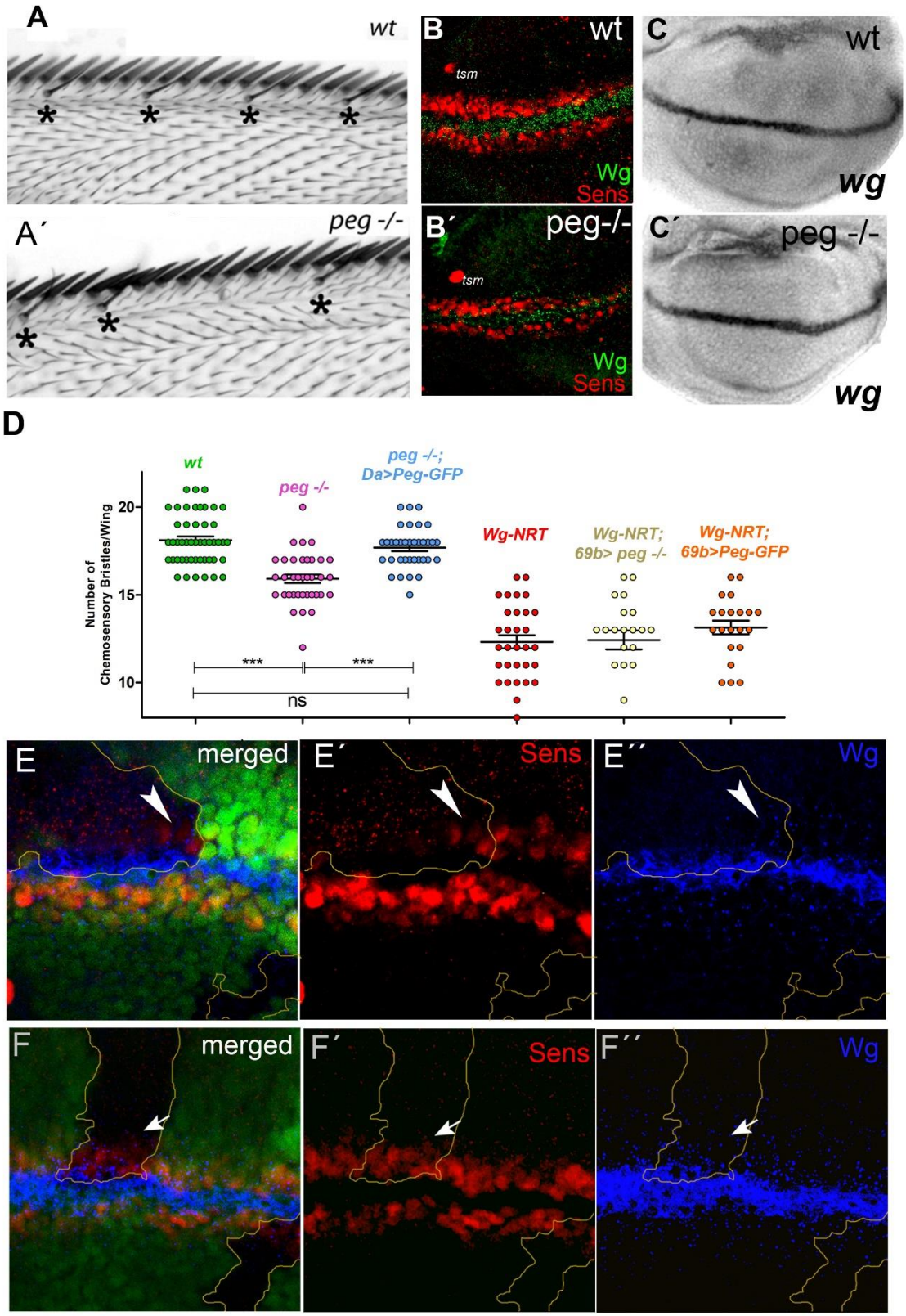

Figure 2

bioRxiv preprint doi: https://doi.org/10.1101/807701; this version posted October 17, 2019. The copyright holder for this preprint (which was not certified by peer review) is the author/funder. All rights reserved. No reuse allowed without permission.

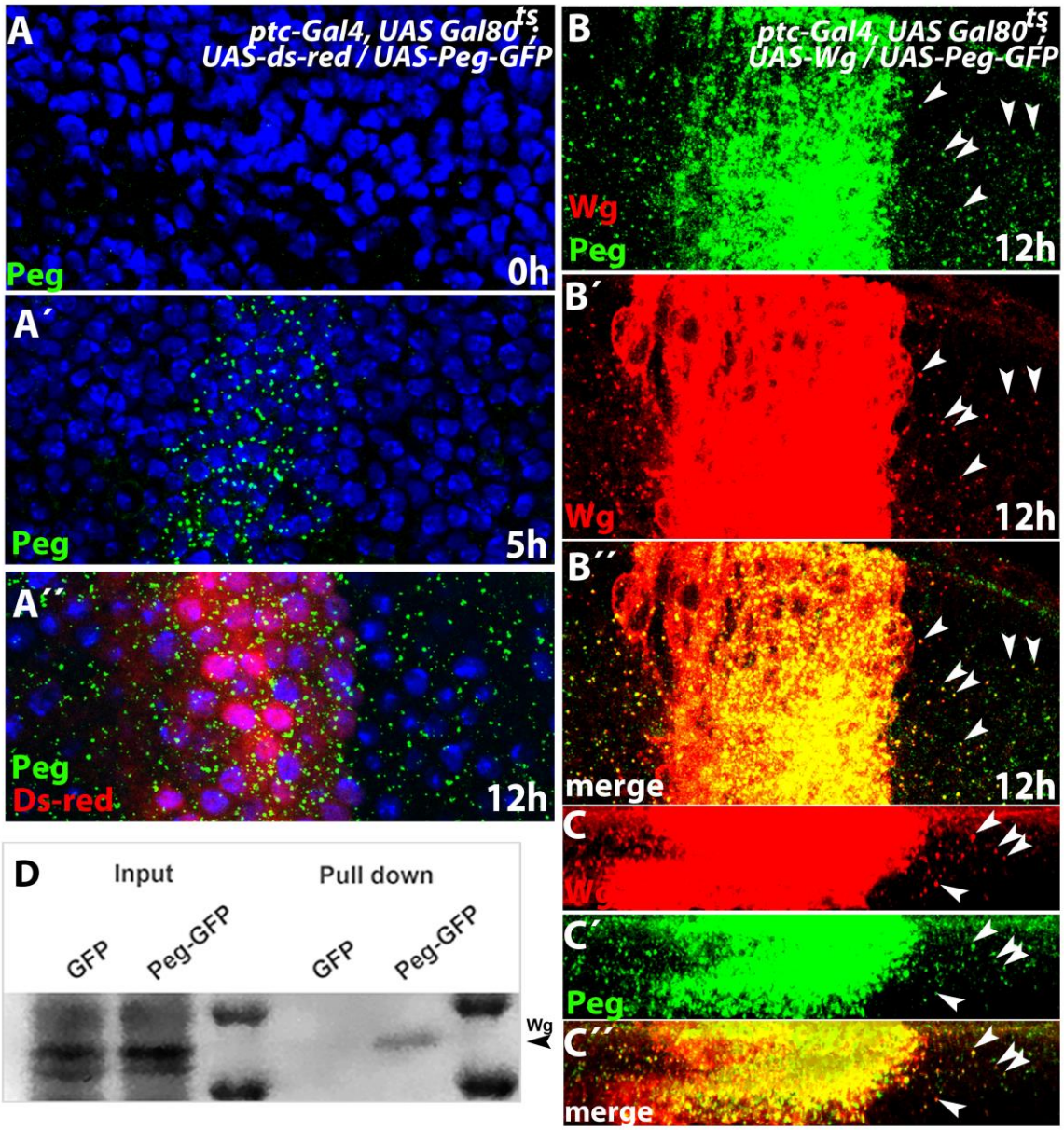

Figure 3

bioRxiv preprint doi: https://doi.org/10.1101/807701; this version posted October 17, 2019. The copyright holder for this preprint (which was not certified by peer review) is the author/funder. All rights reserved. No reuse allowed without permission.

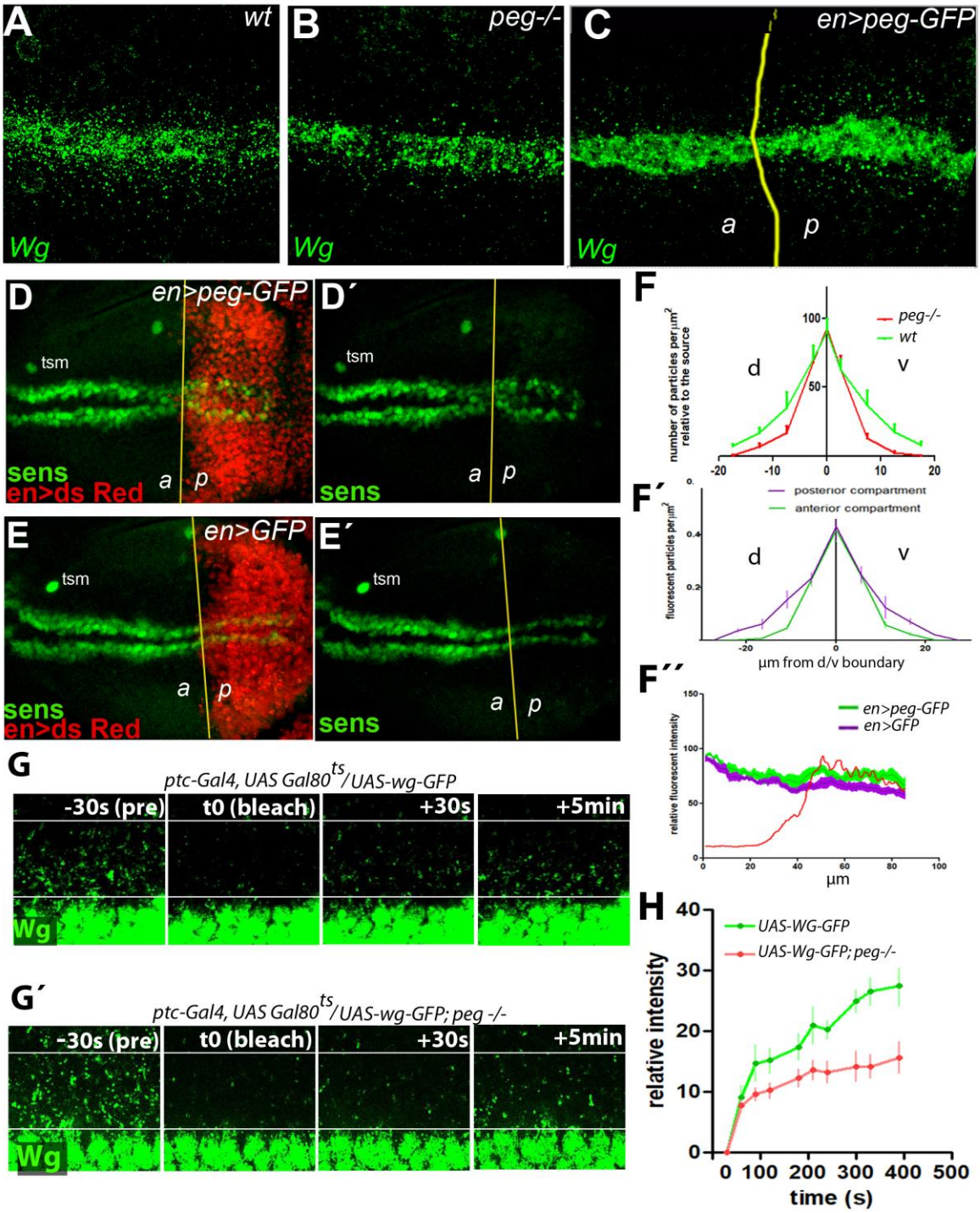

Figure 4

bioRxiv preprint doi: https://doi.org/10.1101/807701; this version posted October 17, 2019. The copyright holder for this preprint (which was not certified by peer review) is the author/funder. All rights reserved. No reuse allowed without permission.

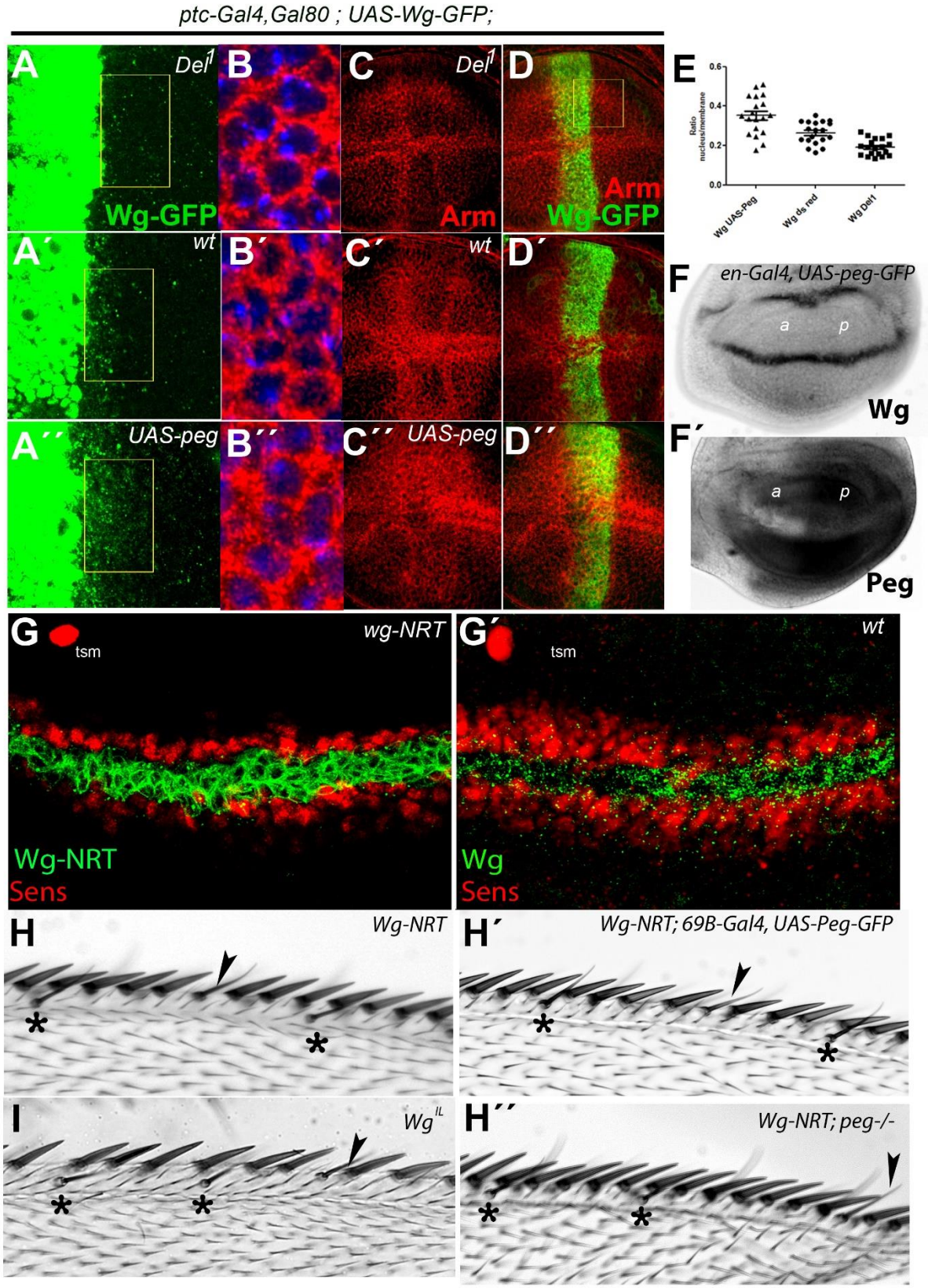

Figure 5

bioRxiv preprint doi: https://doi.org/10.1101/807701; this version posted October 17, 2019. The copyright holder for this preprint (which was not certified by peer review) is the author/funder. All rights reserved. No reuse allowed without permission.

Supplementary Figures

Sup. Figure 1

A-A´´. The expression of *senseless* is significantly reduced in *peg-* mutants and in *wg-NRT* transgenic flies compared to wt. Note that the twin campaniform sensilla (tsm) precursor located some 3-4 cell diameters away from the sens dorsal stripe remains unaffected.

B-B'. Quantification showing (B) the average Sens signal intensity from panels A-A´´, relative to the maximum values. Senseless was quantified in a region of interest, represented by yellow squares in panels A-A´´. 0 µm represents the centre of the *wg*-expressing stripe. (B´) quantification of Wg signal, relative to maximum intensities, from (Fig.4 A´-A´´) over a region of interest adjacent to the Wg expressing cells. 0 µm represents the boundary of Wg expressing cells.

C. Endogenous Wg, revealed with the anti-Wg antibody 4D4, co-localizes with Peg-GFP (arrowheads) expressed in the wing pouch with *rn-Gal4(St Pierre et al., 2002).*

D. Time-line of induction of Peg-GFP expression with *ptc-Gal4-UAS-Gal80^{ts}* by temperature shift (18ºC to 29ºC) prior to dissection shows that Peg-GFP is secreted. The time from induction to dissection is indicated at the right of each set of panels (t).

E. *In-situ* hybridization showing that ectopic expression of Wg using *ptc-Gal4* leads to a downregulation of *peg* in the *ptc* domain (arrowhead), confirming that *wg* negatively regulates the expression of *peg(Butler et al., 2003)* .

Sup. Figure 2

A. Western Blot, from wing imaginal disc extracts showing Wg protein levels in flies over expressing peg-GFP in wing pouch with rn-Gal4, compared to controls expressing GFP with the same driver. Note the higher levels of Wg protein in peg-GFP expressing wing discs.

B. Quantification of the western blot and qPCR data from imaginal discs, comparing the changes in expression between Wg protein and *wg* mRNA. The Wg protein levels were adjusted against total protein loads, and normalized against the GFP only controls. *wg* mRNA levels were obtained using the ΔΔQC values of the *wg* amplicon against the *rp49* control and the experimental conditions against the GFP only controls. All the values were then normalized to controls. Note that even though there are no significant mRNA expression changes between discs over-expressing Peg-GFP and GFP only controls, there is a significant change in protein levels, suggesting that Peg has an effect in Wg stability.

Sup. Figure 3

A. Genomic locus of *peg*, depicting the sites of the *Mi(MIC)02608* transposon and deficiency *Df(3R)BSC680* used to assess initially the viability of *peg* mutant flies. The table shows the number of progeny of each class obtained after crossing heterozygous flies for both the transposon *Mi(MIC)02608* and deficiency *Df(3R)BSC680.* Note the lower number of trans-heterozygous, *Mi(MIC)02608* / *Df(3R)BSC680* progeny.

bioRxiv preprint doi: https://doi.org/10.1101/807701; this version posted October 17, 2019. The copyright holder for this preprint (which was not certified by peer review) is the author/funder. All rights reserved. No reuse allowed without permission.

B. Model of *wg* and *peg* function during the development of the fly wing. During Early-mid third instar (aprox. 84 to 96 h. AEL), Wg protein is present in a developing pattern that transitorily reaches the entire developing wing (Couso et al., 1993b; Couso et al., 1995; Diaz-Benjumea and Cohen, 1993; Klein and Arias, 1998) and maintains the expression of the *vestigial* gene (*vg*), which is required for the growth of the wing cells. Later, from 96 to 132h AEL, *wg* is expressed only at the presumptive wing margin and is required for its development (see Couso et al. 1994 and references therein). Wg activates the expression of proneural genes such as *sens* (this work) and *ac* at both sides of the *wg*-expressing cells, with an effective range of diffusion of 3-4 cells. Amongst the proneural field, individual cells are selected by a Notch-mediated lateral inhibition process to become the precursors of the wing margin bristles. Chemosensory precursors are determined first by about 120h AEL, and mechanoreceptors later. Complete removal of Wg function from 96h AEL eliminates the entire wing margin (see also (Piddini and Vincent, 2009)), whereas later and/or partial removal of Wg reduces the number of chemoreceptors, and then of mechanoreceptors. Peg is required for this process, by being secreted and binding Wg directly it helps Wg effective diffusion up to 3-4 cell away (this work). Loss of Peg reduces the effective range of Wg diffusion to 1-2 cells and produces a mild loss of Wg function phenotype, whereas Wg-NRT reduces it even further (to 1 cell) and produces a stronger, but still not total, loss of Wg function phenotype (Figs. 2 and 5). (see (Phillips and Whittle, 1993) and Couso et al. 1994 (Couso et al., 1994) for *wg* wing margin phenotypes). The effective range of Wg diffusion during wing margin development is indicated by the tsm twin sensilla, which is located some 6-8 cells from the *wg*-expressing cells and is not dependant on Wg function (this work; see also Phillips and Whittle 1993).

bioRxiv preprint doi: https://doi.org/10.1101/807701; this version posted October 17, 2019. The copyright holder for this preprint (which was not certified by peer review) is the author/funder. All rights reserved. No reuse allowed without permission.

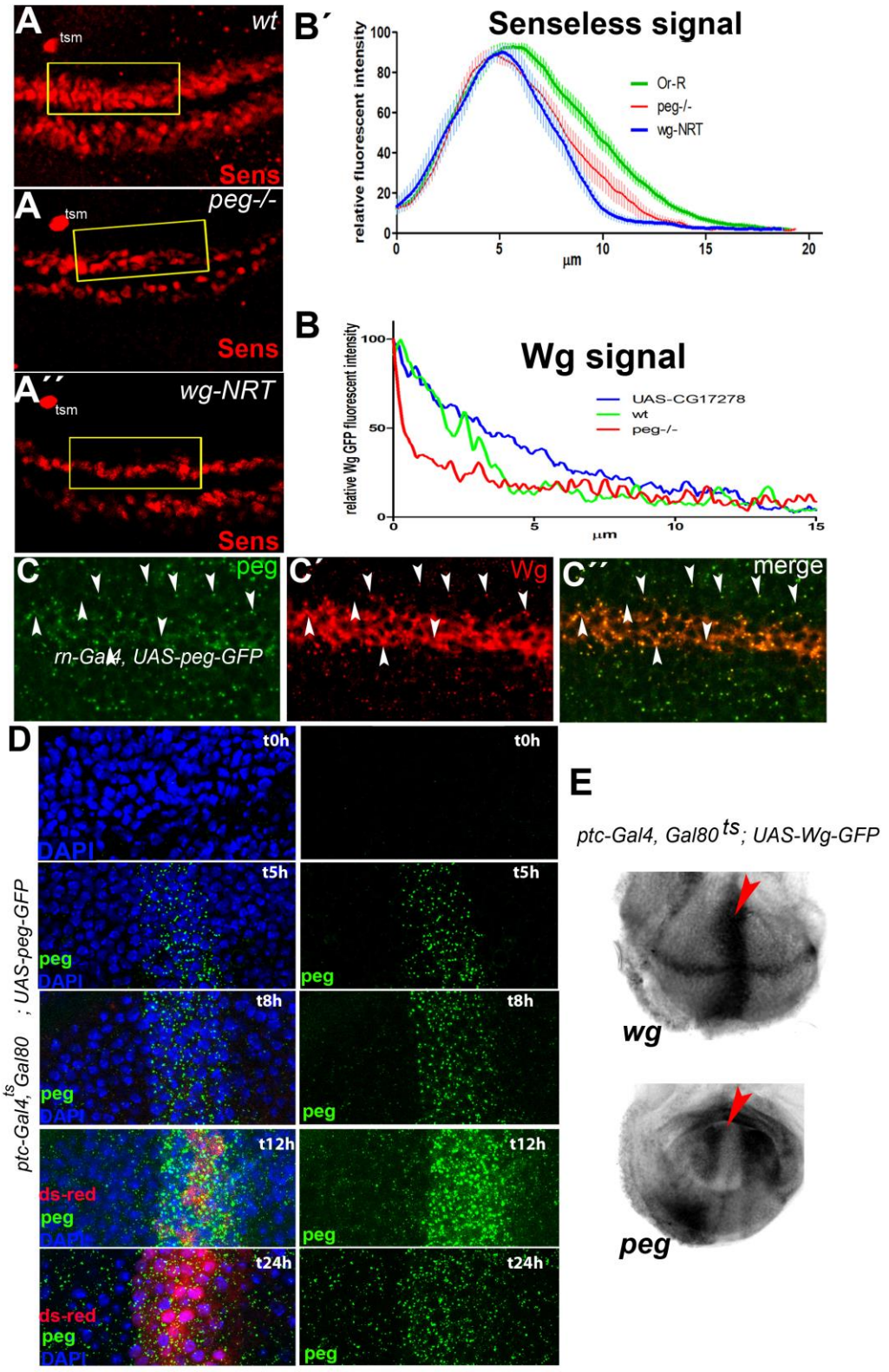

Sup. Figure 1

bioRxiv preprint doi: https://doi.org/10.1101/807701; this version posted October 17, 2019. The copyright holder for this preprint (which was not certified by peer review) is the author/funder. All rights reserved. No reuse allowed without permission.

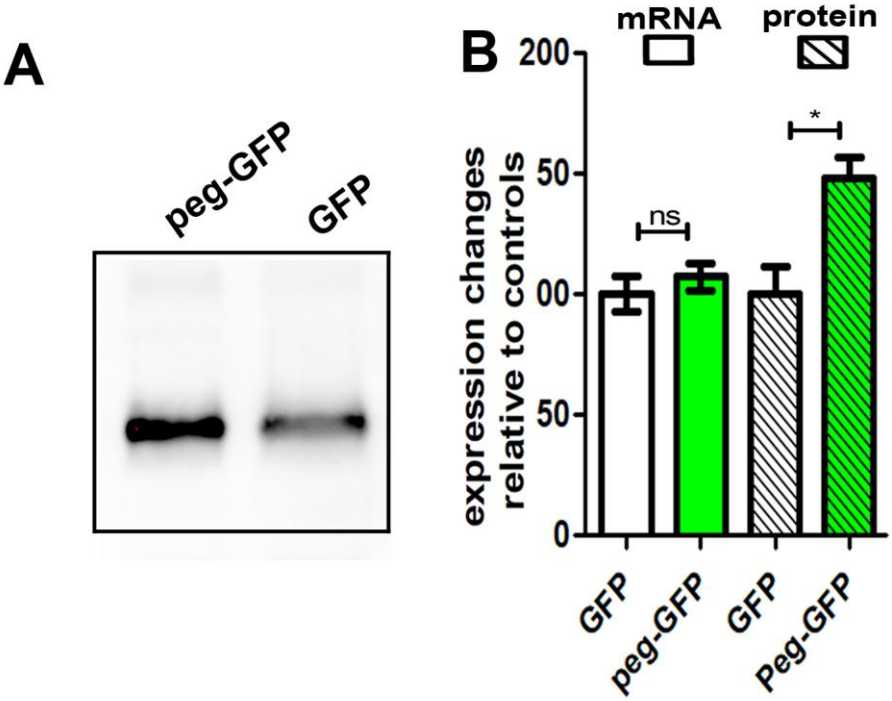

Sup. Figure 2

bioRxiv preprint doi: https://doi.org/10.1101/807701; this version posted October 17, 2019. The copyright holder for this preprint (which was not certified by peer review) is the author/funder. All rights reserved. No reuse allowed without permission.

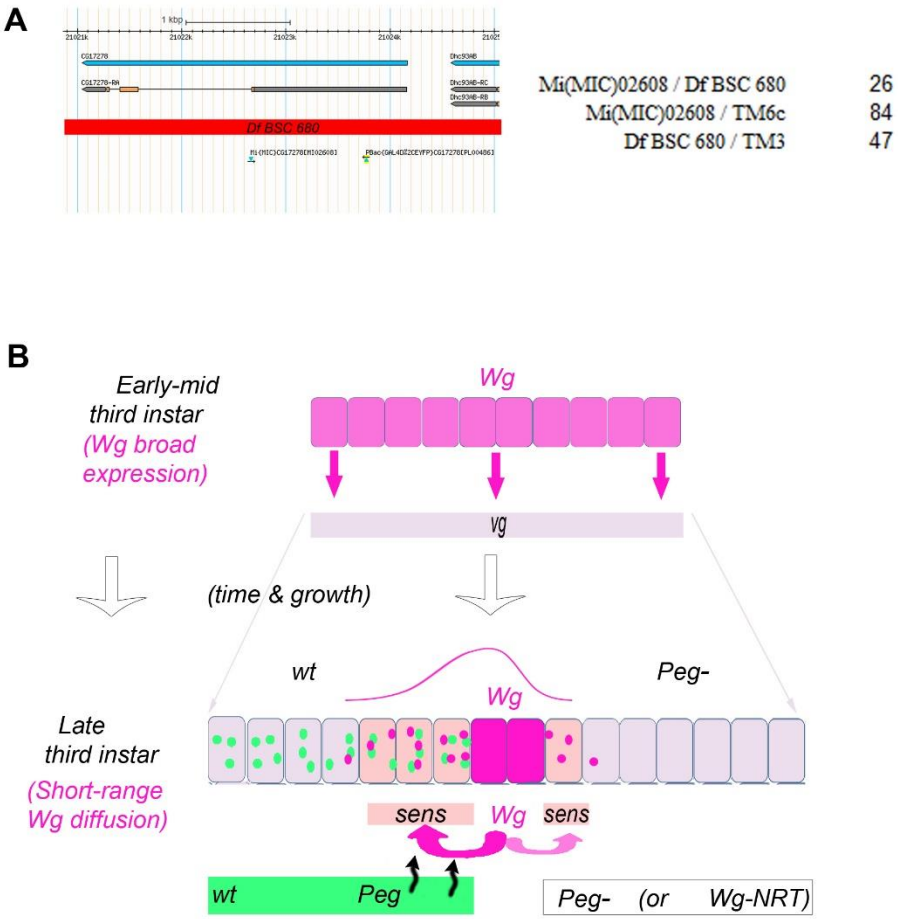

Sup. Figure 3